Surface Selective Polymerization of Polypyrrole on Ordered Mesoporous Carbon: Enhancing Interfacial Conductivity for Direct Methanol Fuel Cell Application

Yeong Suk Choi,[†] Sang Hoon Joo,[†] Seol-Ah Lee,[†] Dae Jong You,[†] Hansu Kim,[‡] Chanho Pak,*,[†] Hyuk Chang,[†] and Doyoung Seung[†]

Energy Lab and Materials Center, Samsung Advanced Institute of Technology (SAIT), P.O. Box 111, Suwon 440-600, Korea

Received November 7, 2005; Revised Manuscript Received March 7, 2006

ABSTRACT: Ordered mesoporous carbon (OMC) selectively covered on the outer surface with polypyrrole (PPy) was prepared by removing the mesoporous silica template after the polymerization of pyrrole adsorbed on the surface of mesoporous silica−carbon composite. The amounts of PPys loaded on OMCs increased with the polymerization time and adsorption time. The resulting PPy−OMC composite maintained regular mesopore structure and high surface area of the OMC. The electrical resistance of PPy−OMC showed a lower value than that of pristine OMC; however, at high loading amount of PPy, the resistance rised to the value of pristine OMC. The PPy−OMC was successfully used as supports for Pt metal particles with a size of 2.8 nm, which illustrated that inner pores of the OMC were effectively utilized for supporting Pt catalyst particles even in the presence of PPy. Furthermore, the electrochemically active surface area obtained from the cyclic voltammogram of Pt catalyst loaded in the PPy−OMC was much higher than that of a commercial catalyst. The Pt-loaded PPy−OMC catalyst exhibited 50% enhanced power density compared to the commercial Pt catalyst in a direct methanol fuel cell (DMFC) single cell test. These results indicated that the PPy−OMC could afford plenty of surface area for supporting the Pt particles in the mesopores, and the Pt particles in PPy−OMCs were applicable to direct methanol fuel cells.

Introduction

Since the first synthesis of ordered mesoporous carbon (OMC) in 1999,[1] considerable research efforts have been devoted to the field of OMCs.[2] OMCs are typically synthesized by using ordered mesoporous silica (OMS) as sacrificing templates via nanotemplating route. The synthesis of OMCs consists of the following steps: infiltration of the OMS templates with appropriate carbon precursors, pyrolysis of the precursors under an inert atmosphere to result in rigid carbon structures within the pores of OMS templates, and subsequent removal of the OMS templates using acidic (e.g., hydrofluoric acid) or basic (e.g., sodium hydroxide) solution. The resulting mesoporous carbons, which are constructed with a regular array of uniform nanopores, exhibit high BET surface areas, uniform pore diameters, large adsorption capacities, and high thermal, acid−base, and mechanical stabilities. Furthermore, the OMCs can be synthesized with wide varieties of pore connectivities,[3] pore sizes,[4] and framework structures[5] depending on the pore structures and diameters of OMS templates and carbon precursors.

In parallel with syntheses of new carbon structures, appealing structural characteristics of OMCs triggered their promising applications as catalyst supports for fuel cells,[3b,6] electrochemical double-layer capacitors,[7] adsorbents,[8] and new inorganic templates.[9] In view of applications, the introduction of functional moieties baring specific reactivity or affinity to the surface of porous carbons in a precise and selective manner is of prime importance. In this regard, the surface modifications of porous

carbon materials have been a subject of great interest toward advanced applications such as adsorbents and catalyst supports.[10−12]

The pore surface of OMCs has three distinctive areas: outer surfaces of OMC particles, mesopore (2−50 nm) surfaces surrounded by carbon rods, and surface of micropores (less than 2 nm) contained in carbon rods of OMC. Modifications of OMCs can be categorized as (1) altering inner pore surfaces with modifiers, (2) filling or coating mesopores and micropores in carbon rods of OMCs, and (3) modifying outer surfaces. A few papers concerning the functionalizations of OMCs have recently begun to appear. Most of the modification methods were associated with functionalizing the surfaces of OMCs via formation of covalent bondings using modifiers such as the Mn−Salen complex[13] and diazonium salts[14] and via fluorination.[15] Polymer-based modifications, however, have rarely been reported yet. Some significant methods related to polymer-based modifiations are summarized as follows. Ryoo and co-workers developed a synthetic route that the nanorods in OMC particles were uniformly coated with polymeric entities to result in mesoporous carbon−polymer composite materials.[16] In another report by Pinnavaia et al.,[17] polypyrrole (PPy) was intercalated inside the mesopores of OMC, but the resulting PPy-intercalated OMCs had decreased electrical conductivities and mesopore sizes with increasing PPy amounts because the PPy, which is less electrically conductive than pristine OMC, occupied the spaces of mesopores. The authors asserted that the electrical conductivity of the OMC needed to be enhanced.

Selective outer surface modification with polymers is rarely reported yet. The purpose of this work is selective modification of OMC surfaces with a conductive polymer for improving surface conductivity of OMCs, while preserving the ordered pore strucutre intact because the ordered mesopores with open

[†] Energy Lab.
[‡] Materials Center.
* To whom correspondence should be addressed: e-mail Chanho.Pak@ samsung.com; Ph +82-31-280-6884; Fax +82-31-280-9359.

Scheme 1. Outlined Representation Illustrating the Synthesis Procedure of Ordered Mesoporous Carbon Covered with Polypyrrole
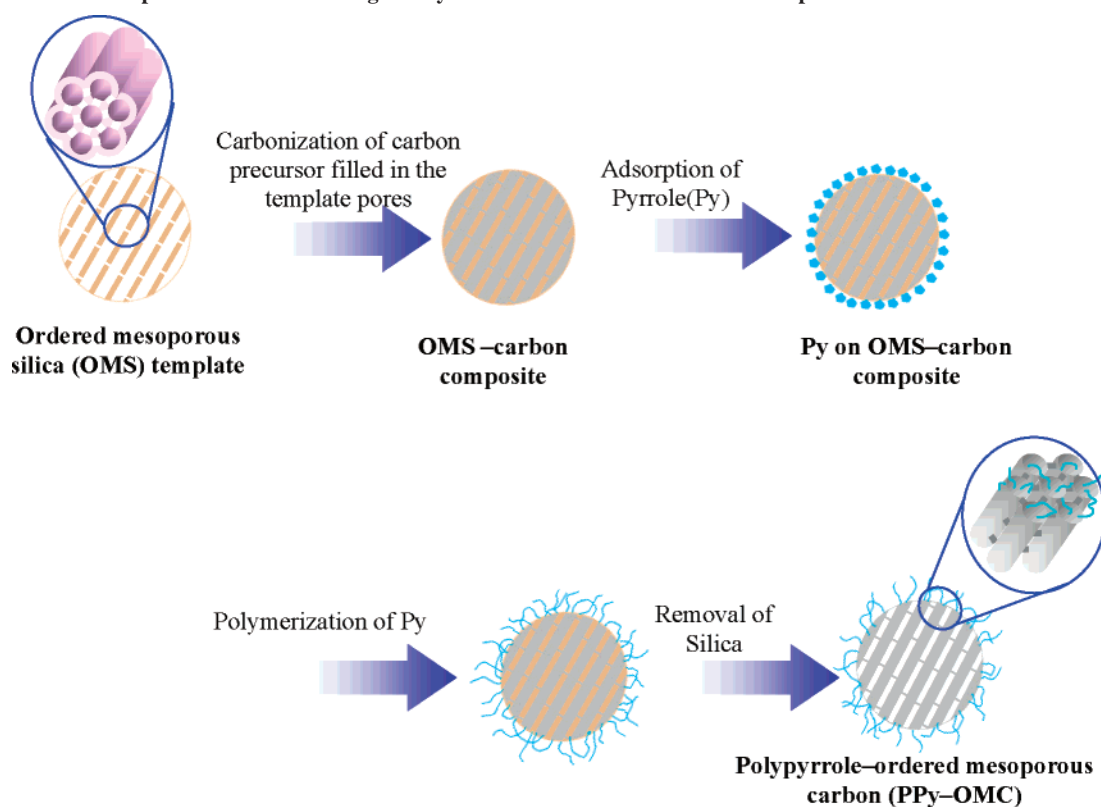
pore structures have strong merits for various applications such as catalyst supports and electrode materials, due to the pore regularity and high surface areas. However, covering outer surfaces of OMCs directly with conductive polymers has been hampered by the fact that general conductive polymers are not soluble in organic solvents but just swollen. Polymerization of monomers is an alternative method for the purpose. Monomers have high diffusion rates with less steric hindrances compared to polymers or supramolecules; thus, monomers can penetrate into micropores (<2 nm) and mesopores ($2-50$ nm) and adsorb on OMC surfaces more easily than polymers or macromolecules.

Herein, we describe a new synthetic route which can selectively functionalize the outer surfaces of OMC particles with conducting polymers, while the internal mesopore structures remain intact, as outlined in Scheme 1. First, a hexagonal OMS−carbon composite was prepared via a reported method:[3a] synthesizing hexagonal OMS templates, filling the mesopores of OMS templates with a carbon precursor, and carbonizing the precursor. Second, the OMS−carbon composite was soaked in an aqueous conductive monomer solution, and then the monomer was polymerized using an oxidant. Third, the silica template in the composite was removed by dissolution in a HF solution to obtain PPy−OMC. Fourth, the conductive polymer on the OMC composite was doped with a dopant. With this method, we expected that, since the polymerization of monomer was performed with the OMS−carbon composite, i.e., prior to the removal of mesoporous silica templates, the monomer can be selectively polymerized on the outer surface of OMC particles; thus, pore sizes and mesostructures of the OMCs would not be deterred after removing silica templates.

We chose pyrrole (Py) as a monomer for conductive polymer because Py is polymerized easily at room temperature and chemically stable under acidic condition after polymerization and PPy has a strong adhesion on solid surface. For example, PPy is used as a coating material of glass surfaces for corrosion

protection and the improvement of glass properties by formation of composites.[19] PPy was also reported to be an alternative carbon source for synthesizing OMCs,[20] where Py monomer was polymerized via a vapor-phase oxidative polymerization in ferric chloride (oxidant)-impregnated mesoporous silica. Since the polymerization is a stoichiometric reaction between Py and ferric chloride, the loading amount of PPy was controlled by the amount of impregnated ferric chloride, resulting in the formation of OMCs. Another reason to choose Py for this work relates to the molecular similarity between carbon and Py. Since the Py has a sp^2 bond character, which is identical with the bonds of carbons or OMCs, Py monomer will be adsorbed on OMC surfaces to form PPy layers. On the other hand, hexagonally ordered CMK-3 type OMC is selected as a carbon framework because the CMK-3 type OMC is reported to be easily synthesized by nanocasting the hexagonal OMS template.[3a]

Experimental Section

Materials. *p*-Toluenesulfonic acid, phenanthrene, acetone, Py, hydrogen peroxide (H_2O_2), sodium hydroxide (NaOH), colloidal silica (Ludox HS-40, 40 wt % SiO_2), P123 block compolymer, acetic acid, hexachloroplatinic acid ($H_2PtCl_6 \cdot 6H_2O$), potassium chloride (KCl), hydrogen perchlorate ($HClO_4$), lithium perchlorate ($LiClO_4$), ethylene carbonate (EC), and propylene carbonate (PC) were purchased from Aldrich Corp. and used without further purification. NaOH and colloidal silica were used for synthesizing a silica source, sodium silicate. Phenanthrene was used as a carbon source for OMC, while *p*-toluenesulfonic acid was used as both carbonization catalyst and carbon source. Py is a conductive monomer, and H_2O_2 is a radical initiator for Py polymerizations. Before polymerization, Py and H_2O_2 were kept in a refrigerator to prevent thermal polymerization and degradation, respectively. $LiClO_4$ was used for doping PPy in the presence of EC/PC. $LiClO_4$, EC, and PC were stored in a glove box to prevent humid contamination. $H_2PtCl_6 \cdot 6H_2O$ was used as a Pt precursor for the preparation of Pt catalyst into mesopores of OMCs. KCl and $HClO_4$

CDV

sample	adsorption time (h)	polymerization time (h)
OMC		
PPy−OMC1	1	1
PPy−OMC2	4	24

were used as electrolytes for electrochemical measurements of Pt-loaded OMC and PPy−OMC.

Preparation of Ordered Mesoporous Silica (OMS), OMS−Carbon Composite, and Ordered Mesoporous Carbon (OMC). The hexagonal OMS template was synthesized from a cost-effective, water-soluble silicate as a silica source and P123 triblock copolymer as a supramolecular template under near-neutral conditions, following the method described by Pinnavaia and co-workers.[18] Sodium silicate solution of Na/Si = 2.5 (10 wt % SiO$_2$) was prepared from colloidal silica Ludox HS-40 (40 wt % suspension in water), NaOH, and deionized water. In the synthesis of OMS templates, P123 triblock copolymer and sodium silicate solution were mixed in deionized water, and then acetic acid diluted with deionized water was added with stirring at ambient temperature in a water-jacketed flask. The resulting gel mixture had a molar composition of 1 SiO$_2$:0.017 P123:2.595 acetic acid:255 H$_2$O. The gel mixture was stirred at 45 °C for 20 h and then placed in an oven at 100 °C for 24 h under static conditions. The silica precipitate was filtered, washed with deionized water, and dried in a freeze-dryer for 48 h. The product was calcined in air at 550 °C for 3 h to remove P123 templates.

The hexagonally ordered OMC was replicated from the above-synthesized OMS template. The carbon precursor solution was prepared by dissolving a 0.7 g of phenanthrene and 2.1 g of *p*-toluenesulfonic acid in 7 mL of acetone. The precursor solution was divided into three portions. After impregnating one portion of the precursor solution into 1 g of the OMS template via incipient wetness, the mixture was dried at 100 °C and successively at 160 °C. The impregnation−drying step was repeated twice more to completely infiltrate the internal pores of the OMS template with the carbon sources. The mixture was subsequently carbonized by heating at 1100 °C for 2 h under nitrogen flow to obtain the OMS−carbon composite. For comparative purposes, OMC without PPy was obtained by dissolving the OMS template from the OMS−carbon composite using 10 wt % aqueous HF solution before the adsorption of Py.

Synthesis of Polypyrrole-Ordered Mesoporous Carbon (PPy−OMC). The OMS−carbon composite was subjected to PPy coating as follows. The composite was immersed in an aqueous Py solution (1 M) for 1 or 4 h. To polymerize the Py monomers adsorbed on the composite surfaces, the composites were immersed in a 30 wt % H$_2$O$_2$ solution for 1 or 24 h. The experimental conditions and sample designations are listed in Table 1. After the polymerization, the composites were filtered, washed with deionized water three times, and dried at 60 °C for 12 h to remove remaining Py monomers. The PPy-covered OMS−carbon composites were then washed with a HF aqueous solution (10 wt %) three times at room temperature to remove silica templates.

After drying, the PPy on OMC surfaces was doped with LiClO$_4$ using EC and PC as solvents. The powder samples were stirred in a 5 wt % LiClO$_4$-EC/PC (1:1 mol/mol) solution for 48 h at room temperature. The doped powders were filtered, washed with deionized water and ethanol successively, and then dried for 5 h at 60 °C under high vacuum.

Preparation of Pt Catalyst with Pristine OMC and PPy−OMC. The carbon-supported Pt catalyst was synthesized via an incipient wetness method. A half gram of pristine OMC was mixed with 1.5 mL of acetone containing Pt precursor, H$_2$PtCl$_6$·6H$_2$O. The amount of H$_2$PtCl$_6$·6H$_2$O in the solution was adjusted to obtain 60 wt % Pt loading. After being dried in an oven at 60 °C overnight, the H$_2$PtCl$_6$-impregnated OMC was heated in a H$_2$ flow to 200 °C and kept for 2 h at the same temperature to reduce H$_2$PtCl$_6$ to Pt metal particles. The adsorbed hydrogen on Pt particles was removed by heating to 350 °C and kept for 2 h under nitrogen flow.

Single Cell Performance of Pt/PPy−OMC in Direct Methanol Fuel Cell (DMFC) Application. Catalyst ink was prepared by dispersing the Pt/PPy−OMC in alcohol solution with Nafion dispersion. The catalyst ink was sprayed onto the gas diffusion layer to form a cathode catalyst layer with 2 mg/cm^2 Pt. The anode catalyst layer was prepared by the same way with the cathode, except the use of PtRu black catalyst (HiSpec 6000 from Johnson Matthey Fuel Cells)[21] of 6 mg/cm^2. The membrane electrode assembly (MEA) was fabricated by hot pressing the cathode and the anode on each side of Nafion 115 membrane. Single cell tests were conducted at 50 °C using the MEA with 10 cm^2 of reaction area and 1 M MeOH and dry air as fuels for the anode and the cathode, respectively. Potential vs current density plots were obtained by potentiodynamic measurements from an open-circuit voltage to 0.2 V.

Characterization. Scanning electron microscopy (SEM) images were obtained with a Hitachi S-4500 field emission scanning electron microscope operating at 20 kV. Transmission electron microscopy (TEM) images were obtained using a G2 FE-TEM Tecnai microscope at an accelerating voltage of 200 kV. X-ray diffraction (XRD) patterns were measured by a Philips X'pert Pro X-ray diffractometer equipped with a Cu Kα source at 40 kV and 40 mA. The nitrogen adsorption experiment was performed at −196 °C using a Micromeritics ASAP 2010 system. Surface areas of the samples were calculated by using the BET equation. Pore size distributions were estimated by Barrett−Joyner−Halenda (BJH) method from adsorption branches of isotherms.

To detect pyrrole on the PPy−OMC, the pyrolysis−gas chromatograph mass spectroscopy (py-GC/MS) technique was carried out at 600 °C using a HP G1530N gas chromatograph. The mass spectrum was obtained using an Agilent 5973N mass spectrometer. Thermogravimetric analyses (TGA) were carried out using a TA Instrument TGA 2050, heating from room temperature to 800 °C at a rate of 10 °C/min under a N$_2$ atmosphere.

Electrical resistance was measured using a Changmin Tech. CMT series JANDEL four-point probe at room temperature. Sample powders were pressed at 75.4 kg/cm^2 for measurements. To measure the electrochemically active surface areas of Pt particles loaded on OMCs, cyclic voltammetries (CV) were recorded on a Solartron 1287A potentiostat at 25 °C. Pt gauze and Ag/AgCl (in saturated KCl) were used as the counter and the reference electrode, respectively. All potentials were reported with respect to a normal hydrogen electrode (NHE). The working electrodes (carbon paper) were brushed with the catalyst inks prepared by suspending the catalyst samples in the alcohol with an ionomer, Nafion dispersion (5 wt %). Aqueous HClO$_4$ solution (0.1 M) was stirred constantly and purged with nitrogen gas. The cyclic voltammetry were performed in a potential range of −0.1 to 1.4 V vs NHE at a sweep rate of 5 mV/s.[22]

Results and Discussion

When PPy was sucessfully polymerized on the surface of OMC, the OMC enveloped by PPy (PPy−OMCs) would have different physical and electrical properties due to the presence of conductive polymer. The presence of PPy on the outer surface of OMC was examined with SEM images. Pristine OMC and PPy−OMCs had aggregated particles that consisted of individual particles of about 300 nm diameters, as shown in Figure 1. In addition to the particles sizes, the SEM images provide surface states of PPy−OMCs. The PPy−OMCs had rougher surfaces than that of pristine OMC, as shown in Figure 1b,c. Particularly, in the case of PPy−OMC2, which was prepared by polymerizing the Py for 24 h, fiber-shaped PPys (indicating bulk PPy) could be found among the OMC particles, as shown in Figure 1c. The roughness of PPy−OMCs was proportional to the adsorption time and the polymerization time.

The internal pore structures of PPy−OMC and pristine OMC were examined using TEM. The TEM image of PPy−OMC1 in Figure 2 shows carbon rods (about 8 nm diameter) and pores
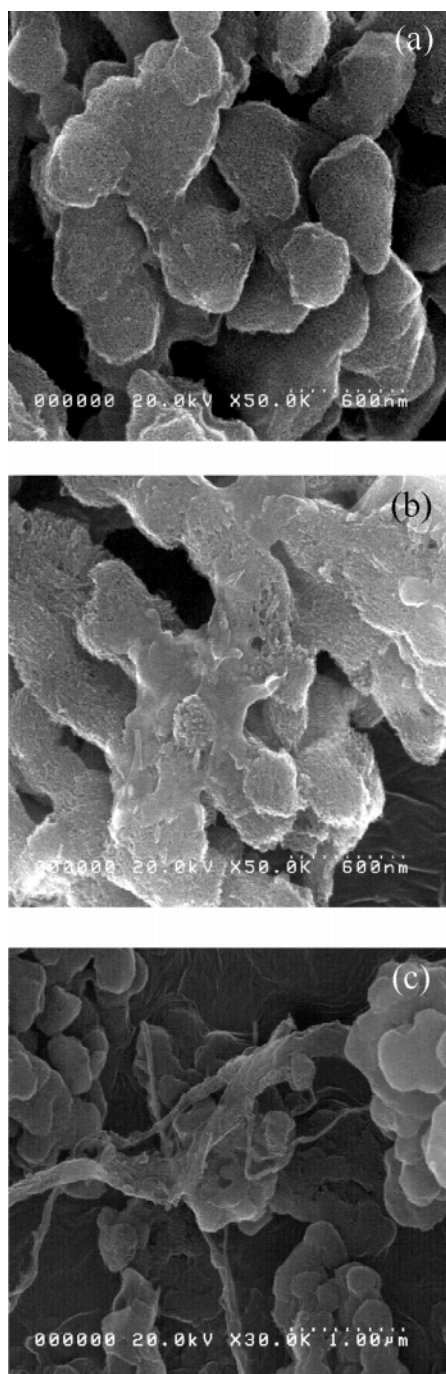
CDV

Figure 1. Typical SEM images of (a) pristine OMC, (b) PPy−OMC1, and (c) PPy−OMC2.

(about 3−4 nm) in an OMC particle, which means that the ordered structure of PPy−OMC was not disturbed by the presence of PPy. The SEM and TEM images exhibit that the PPys were selectively formed in the interfacial areas of OMC particles. The possibility of PPy presence in mesopores of OMC still remains, and this aspect is to be explained in the next section. The presence of PPy in PPy−OMC1 was confirmed with a py-GC/MS technique, as given in Figure 3. The chromatogram of PPy−OMC1 obtained at 600 °C showed a peak at 4 min, which can be assigned to Py.

Thermal properties and loading amounts of PPys were confirmed with thermogravimetric analysis (TGA), as shown in Figure 4. The weight loss of PPy−OMCs in the temperature of 350−450 °C was assigned to thermal decompositions of PPy main chains. The amount of PPy loaded on the OMC was
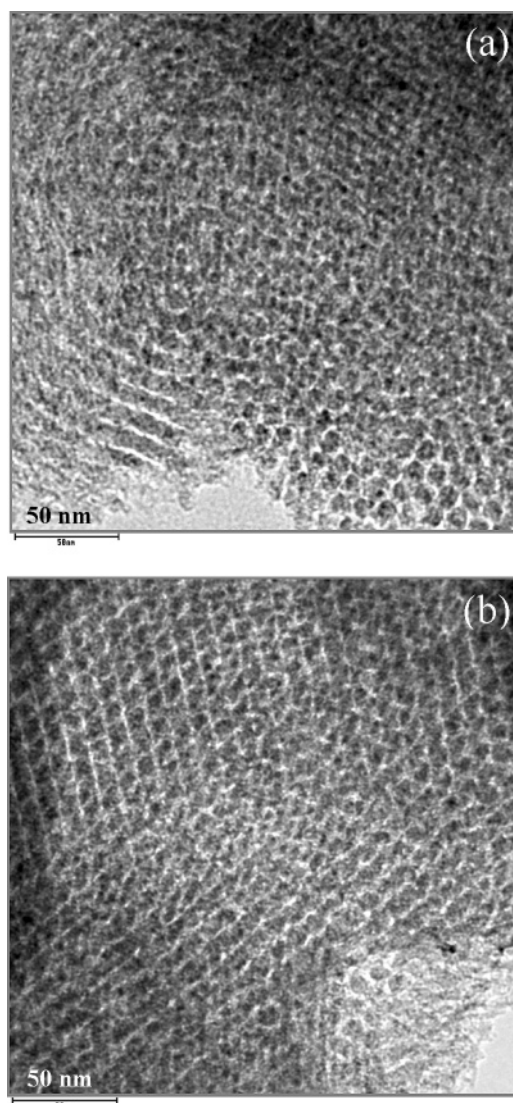

Figure 2. Typical TEM images of (a) pristine OMC and (b) PPy−OMC1.

determined using the residual weight difference between PPy−OMCs and the pristine OMC from TGA traces at 800 °C. The residual weight percentage of pristine OMC at 800 °C was 92.11%, while those of PPy-OMC1 and 2 were 88.16% and 87.88%, respectively. The PPy amounts in the PPy−OMCs, thus calculated, were 3.96% for PPy−OMC1 and 4.23% for PPy−OMC2, respectively. PPy amounts on OMC increased as the polymerization time and adsorption time increased. It is noteworthy that PPy−OMC2 showed a broad weight loss trace compared to PPy−OMC1 in the temperature range. The broadness of TGA trace from PPy−OMC2 might be related with a wide molecular weight distribution of PPy. Generally, molecular weights and their distributions of polymers become low and wide with the amounts of initiators, and the conversions of monomers to polymers increase as the polymerization times increase. The Py monomer on PPy−OMC2 was polymerized for a longer time, 24 h, with excessive oxidant, compared with PPy−OMC1. Therefore, the PPy on PPy−OMC2 might have a wide molecular weight distribution, resulting in the broad TGA trance and a high amount of PPy.

The primary goal of this work was to increase interfacial conductivity of OMCs without sacrificing high surface area and pore volume of the pristine OMC, so we further investigated the possibility of structural deformation or pore shrinkages due
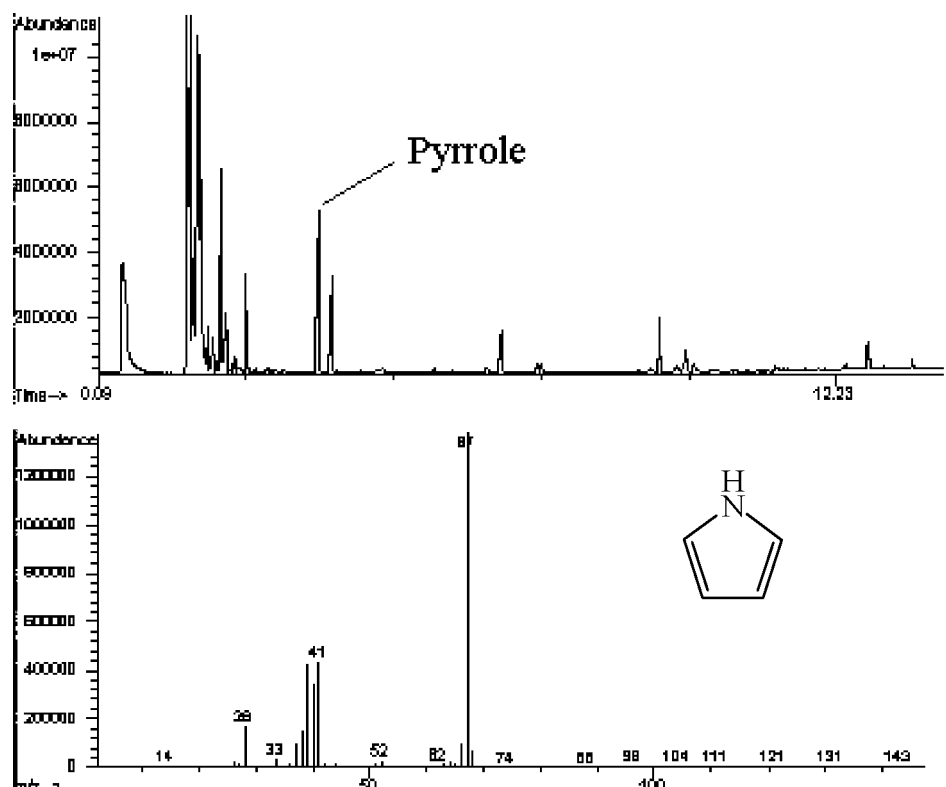
CDV

Figure 3. Pyrolysis−gas chromatograph mass spectroscopy of PPy−OMC1 (top) and analysis result of the peak eluded at 4 min (bottom).
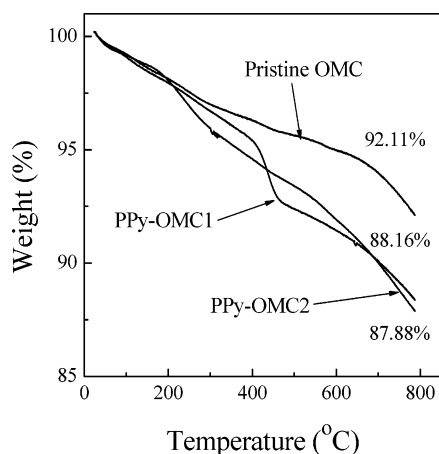

Figure 4. Thermogravimetric analysis curves for PPy adsorbed on OMC under a nitrogen atmosphere.

to the PPy polymerization using XRD and nitrogen adsorption. Figure 5a displays XRD patterns of pristine OMC and PPy−OMCs. The XRD of pristine OMC exhibited well-resolved three peaks, which could be assigned to (100), (110), and (200) peaks of the 2-D hexagonal *p6mm* space group, as reported earlier.[3a] Although OMC surfaces were covered with PPy, the PPy−OMCs exhibited nearly the same XRD patterns as the pristine OMC did, without any significant change in peak intensity or position. The *d*-spacings of the (100) peak of both pristine OMC and PPy−OMCs, calculated with the Bragg equation, were 9.7 nm. Generally, the inclusion of guest species into the internal pores of mesoporous materials results in the decrease in the peak intensity.[17] This result, therefore, indicates that most of the PPys existed outer surface of OMC particles, rather than located inside the mesopores, while maintaining the open mesoporous structure of OMC.

The open pore system of PPy−OMCs can be clearly confirmed by nitrogen adsorption isotherms and corresponding pore size distributions, as shown in Figure 5b,c. The OMS template had 10.5 nm pores, which would be filled with a carbon precursor, phenanthene, to become carbon rods after carbonization. Surface areas of the samples were calculated by using the BET equation, and pore size distributions were estimated by the BJH method from adsorption branches of isotherms. The isotherm of the OMC was nearly preserved after the PPy polymerization, except for the slight decrease in nitrogen uptakes. Furthermore, the pore sizes of PPy−OMC samples were the same with the pristine OMC, as the distribution curves of both samples centered at 4.0 nm shown in Figure 5c, confirming the open mesopores of PPy−OMCs without clogging with PPy. The BET surface area and pore volume of hexagonal OMS template, calculated from N_2 adsorption data, were 559 m^2/g and 1.45 cm^3/g, respectively. The BET surface areas and pore volumes of pristine OMC and PPy−OMCs were as follows: 845 m^2/g and 0.87 cm^3/g for pristine OMC, 801 m^2/g and 0.83 cm^3/g for PPy−OMC1, 795 m^2/g and 0.86 cm^3/g for PPy−OMC2. The slight decrease in surface areas between pristine OMC and PPy−OMCs might be related to slight covering of the entrances of mesopores by PPy. The XRD patterns and nitrogen adsorption data suggest that the PPys were exclusively present on the OMC outer surfaces. It should be noted that, in the work by Kim et al., where the OMC was intercalated with PPy, the polymer intercalation was accompanied by the decrease in pore sizes due to the occupied PPy in the internal pores of OMC.[17]

The surface-selective polymerization of Py was expected to induce the alternation of electrical properties of OMCs. To address this point, the electrical resistances of PPy−OMCs were measured using a four-point probe method. Figure 6 shows electrical resistances of pristine OMC and PPy−OMCs doped with LiClO$_4$. The electrical resistance of the pristine OMC was
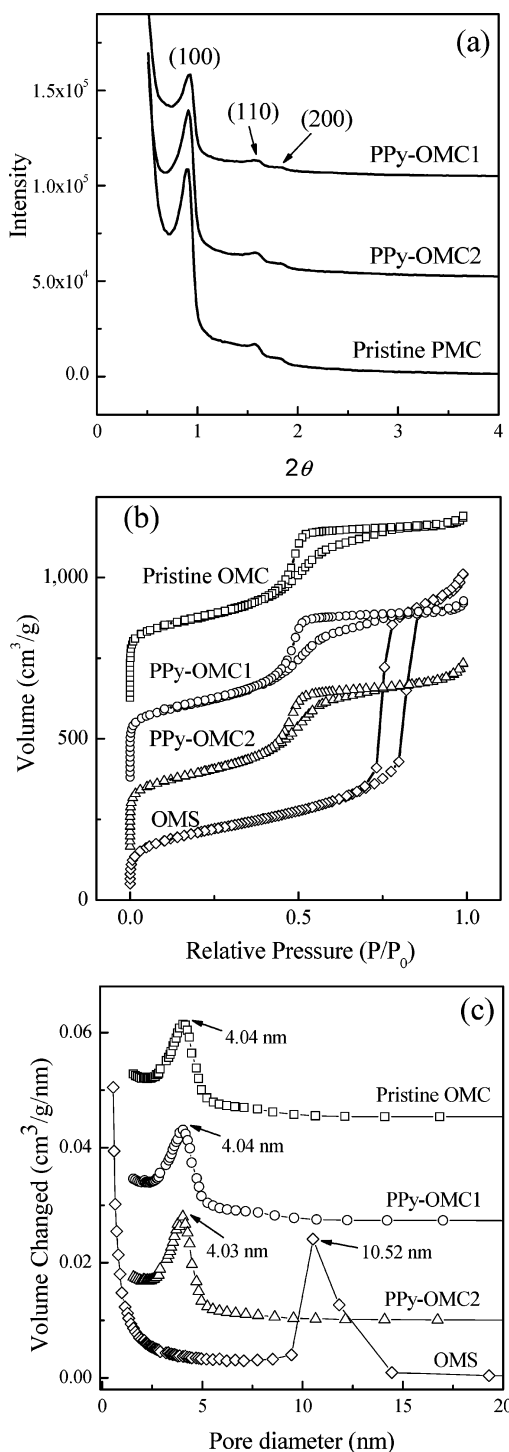
CDV

Figure 5. (a) Powder XRD patterns of pristine OMC and PPy−OMCs. (b) N_2 adsorption−desorption isotherms at −196 °C for pristine OMC, PPy−OMCs, and hexagonal OMS template. The adsorption−desorption isotherms of samples were vertically shifted upward 250, 500, and 750 cm^3/g for PPy−OMC2, PPy−OMC1, and pristine OMC, respectively. (c) Pore size distributions estimated by the BJH method from adsorption branches.

Figure 6. Interfacial electrical resistance of pristine OMC and PPy− OMCs after doping with $LiClO_4$.
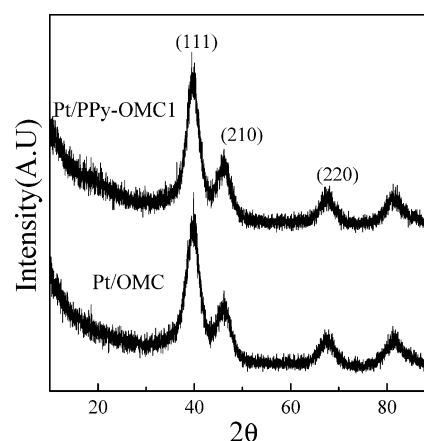
Figure 7. XRD patterns of Pt catalyst loaded in pristine OMC and PPy−OMC.

112 $m\Omega/cm^2$. The resistance value of PPy−OMC1 after doping decreased by 52.7% to 53 $m\Omega/cm^2$. As the PPy polymerization time increased (PPy−OMC2), the resistance rised to the value of pristine OMC. The resistance data indicate that the interfacial resistance of OMC was reduced by the coated PPy, and the resistance was inversely proportional to the PPy polymerization times or the PPy amounts. The resistance drop of PPy−OMC1 can be explained as follows: the PPys could connect the OMC
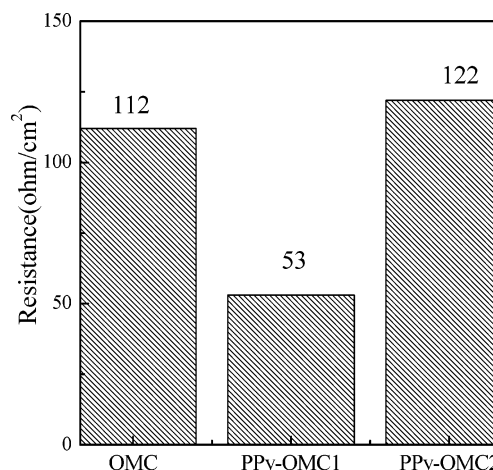
particles during the polymerization, and the connecting PPy acted like an electrical bridge between adjacent OMC particles at a low amount of PPy, thus lowering the interfacial resistance. However, at high loading amount of PPy, the bulk PPy increased the resistance because the PPy itself has higher resistance value than OMC.[17]

Lowering the interfacial electrical resistance of the OMC without deterioration of mesopores by PPy molecules brought up the possibility of utilizing the PPy−OMC for supporting metals such as Pt to apply for the fuel cell catalyst. To examine the possibility, a Pt precursor solution, $H_2PtCl_6 \cdot 6H_2O$ in acetone, was impregnated into the mesopores of pristine OMC and PPy− OMC1 and reduced with H_2 gas to make Pt particles, as described in the Experimental Section. The amount of Pt loaded in OMCs was controlled to about 60 wt % in the total weight. The XRD patterns of Pt loaded in pristine OMC and PPy− OMC1 were obtained, as shown in Figure 7. The Pt loaded in pristine OMC showed diffraction patterns at 39.96°, 46.22°, and 67.59°, which were assigned to (111), (210), and (220) planes of Pt with reference to the JCPDS (Joint Committee on Powder Diffraction Standards) card. These diffraction peaks indicate that face-centered-cubic (fcc) Pt metal particles were formed in the OMC particles. The average crystalline size of Pt, calculated using the Scherrer's equation, was 2.5 nm.[23] The Pt loaded in PPy−OMC1 showed the same diffraction patterns that were observed in the XRD patterns of the Pt loaded in pristine OMC, and the average crystalline size was 2.8 nm.
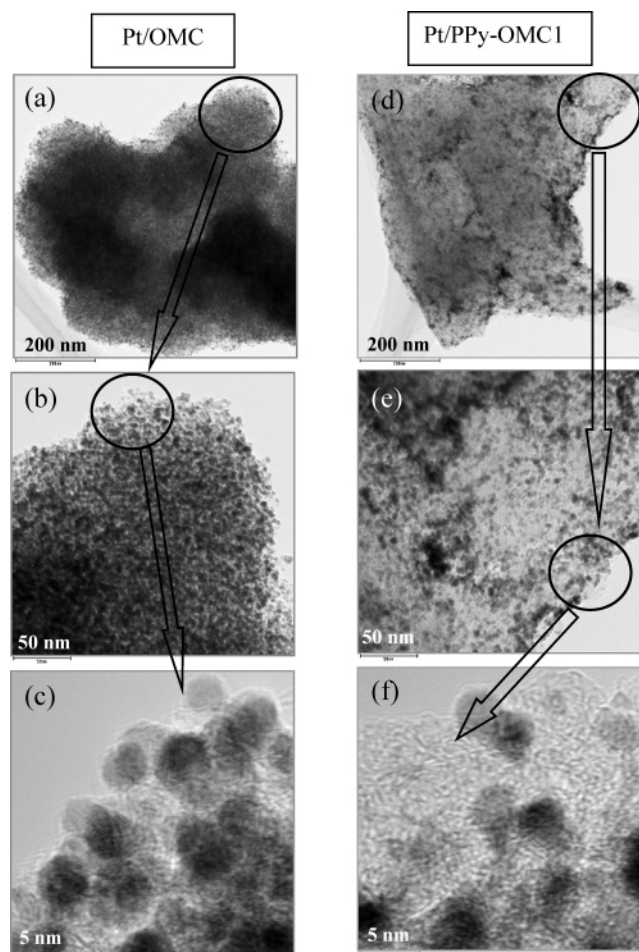
CDV

Figure 8. Typical TEM images of pristine OMC (left) and PPy−OMC1(right) loading Pt catalyst in the pores.
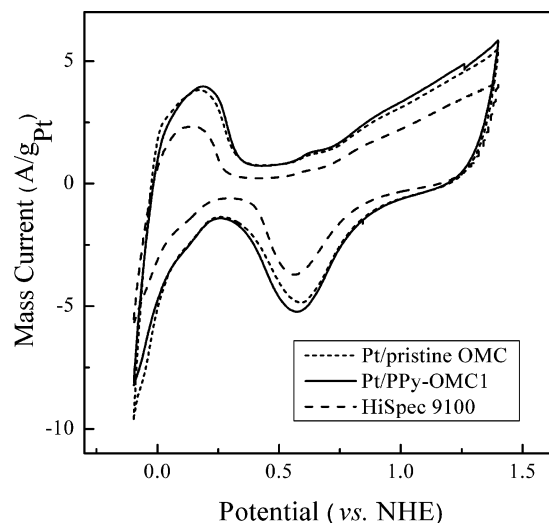

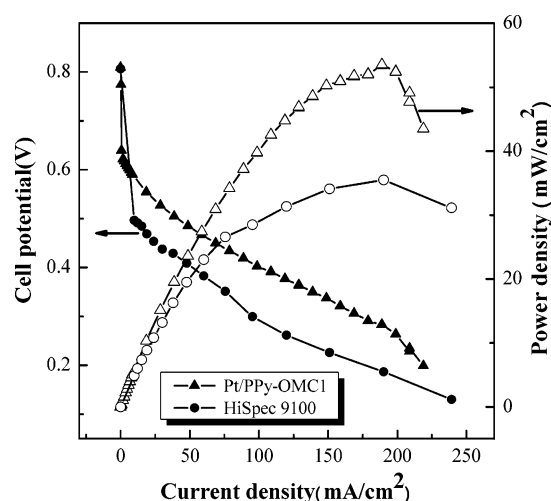**Figure 9.** Cyclic voltammograms of the Pt loaded in pristine OMC, PPy−OMC1, and HiSpec 9100.

Figure 10. Polarization curves of DMFC single cells consisted of Pt/PPy−OMC1 and HiSpec 9100 as cathode catalysts.

The morphology and the shape of the Pt particles were observed with TEM images, as shown in Figure 8. The TEM image shows that round Pt particles were distributed in the mesopores of pristine OMC. The Pt particle size in PPy−OMC1 was about 3 nm, and the size was consistent with the value obtained from the XRD patterns. In the highly magnified TEM image as shown in Figure 8f, the PPy−OMC1 had brighter interfacial areas that were not observed in the pristine OMC as displayed in Figure 8e, and also Pt particles were rarely deposited in these areas. These areas might be the PPy, which were selectively polymerized on the outer surface of OMC. The XRD patterns and TEM images of Pt particles illustrate that, despite the presence of PPy, inner pores of PPy−OMC1 were effectively utilized for supporting Pt particles.

Electrochemical measurements were made using a three-electrode cell at 25 °C. Figure 9 shows the CVs of Pt catalysts loaded in pristine OMC and PPy−OMC1. Broad CV curves assigned as hydrogen adsorption and desorption appeared in a voltage range of −0.1 to 0.4 V. The broad CV curves indicate that the Pt particles in both pristine OMC and PPy−OMC1 were polycrystalline, containing a mixed facet of fcc Pt particles. Electrochemically active surface areas of the Pt particles in the OMCs were obtained from the total charge amounts required for the hydrogen desorption area of CV curves and from the Pt particles surfaces assuming a value of 210 μC/cm^2 for the oxidation of atomic hydrogen.[22] The active surface areas of the Pt loaded in both OMCs were almost the same value, 71.2 m^2/g for pristine OMC and 73.9 m^2/g for PPy−OMC1. The electrochemically active surface area of a commercial Pt catalyst

supported in an activated carbon, HiSpec 9100 of Johnson Matthey Fuel Cells, was also measured as a reference. According to the data sheet provided by the Johnson Matthey Fuel Cells,[21] the HiSpec 9100 had a maximum 2.8 nm of Pt particles in activated carbons, and the Pt loading in the carbon was maximum 58.5%. These values are very similar to those from the Pt supported on PPy−OMC1. However, the active surface areas of the Pt loaded in active carbon (HiSpec 9100) was 42.3 m^2/g. The active surface areas of Pt loaded in pristine OMC and PPy−OMC1 were much larger than that of HiSpec 9100. High active surface areas of Pt loaded in OMCs might be related with the high surface area from the mesopore and higher pore volumes of OMCs. The active surface areas of Pt suggest that the PPy−OMC could afford large surface area for supporting the Pt particle in the mesopores and more accessible Pt particles as an effective support because PPy was adsorbed only on the outer surface of OMC.

To probe the benefit of highly dispersed Pt catalyst, the DMFC performance tests were made with a 10 cm^2 single cell having two catalysts (Pt/PPy−OMC1 and HiSpec 9100) as cathode electrocatalysts under the same conditions. As illustrated in Figure 10, the single cell with the 60 wt % Pt/PPy−OMC1 catalyst exhibited better performance than that of HiSpec 9100. The current densities at 0.4 V and 50 °C were 99.5 and 52.7

CDV

mA/cm^2 for Pt/PPy−OMC1 and HiSpec 9100, respectively. Apparently, Pt/PPy−OMC1 catalyst achieved a much higher electrocatalytic activity compared to the HiSpec 9100. The particle size and the loading amount of Pt in HiSpec 9100 were nearly identical with the Pt in PPy−OMC1. Thus, the power density data illustrate that the uniform distribution of Pt in the PPy−OMC1 contributed to the increasing the single cell performance, and the high pore volume of the OMC provides enough surface area for anchoring Pt particles. It is worth to notify that high performance was obtained in the presence of considerable methanol crossover from the anode side, in which highly dispersed Pt/PPy−OMC1 catalyst also promote methanol oxidation in the cathode even more than that of HiSpec 9100.

Conclusion

A synthetic strategy, which selectively functionalized the outer surfaces of OMC, has been presented. The PPy−OMC composite material maintained the regular mesopore structure and the high surface area of the OMC, while exhibiting decreased electrical resistance. Preservation of the regular mesopore structure and the high surface area of the OMC after PPy functionlization was confirmed by loading of highly dispersed Pt catalyst. The electrochemically active surface area of the Pt catalyst loaded in the PPy−OMC was about 50% higher than that of a commercial catalyst (HiSpec 9100). The Pt-loaded PPy−OMC catalyst exhibited 50% enhanced power density compared to the commercial Pt catalyst in a DMFC single test. These results indicated that the PPy−OMC could afford plenty of surface area for supporting the Pt particles in the mesopores compared with a commercial Pt catalyst loaded on activated carbons. Thus, the selective PPy polymerization on OMC surfaces proved to be a new modification method of OMCs for improving electrical properties such as interfacial electrical resistances without altering the ordered structures of OMC. The open mesopore structure, in combination with reduced the electrical resistance, of the PPy−OMC system would be advantageous for the application of OMCs as materials for fuel cells and Li ion batteries. We expect that the selective functionalization method reported herein would be extended to mesoporous carbons with various pore topologies and pore size ranges and other conducting polymers.

References and Notes

(1) Ryoo, R.; Joo, S. H.; Jun, S. *J. Phys. Chem. B* **1999**, *103*, 7743.
(2) (a) Ryoo, R.; Joo, S. H.; Kruk, M.; Jaroniec, M. *Adv. Mater.* **2001**, *13*, 677. (b) Ryoo, R.; Joo, S. H. *Stud. Surf. Sci. Catal.* **2004**, *148*, 241. (c) Lee, J.; Han, S.; Hyeon, T. *J. Mater. Chem.* **2004**, *14*, 478.
(3) (a) Jun, S.; Joo, S. H.; Ryoo, R.; Kruk, M.; Jaroniec, M.; Liu, Z.; Ohsuna, T.; Terasaki, O. *J. Am. Chem. Soc.* **2000**, *122*, 10712. (b) Joo, S. H.; Choi, S. J.; Oh, I.; Kwak, J.; Liu, Z.; Terasaki, O.; Ryoo, R. *Nature (London)* **2001**, *412*, 169. (c) Che, S.; Garcia-Bennett, A. E.; Liu, X.; Hodgkins, R. P.; Wright, P. A.; Zhao, D.; Terasaki, O.; Tatsumi, T. *Angew. Chem. Int. Ed.* **2003**, *42*, 3930. (d) Kleitz, F.; Choi, S. H.; Ryoo, R. *Chem. Commun.* **2003**, 2136. (e) Kim, T.-W.; Ryoo, R.; Gierszal, K. P.; Jaroniec, M.; Solovyov, L. A.; Sakamoto, Y.; Terasaki, O. *J. Mater. Chem.* **2005**, *15*, 1560. (f) Lee, J.; Yoon, S.; Oh, S. M.; Shin, C. H.; Hyeon, T. *Adv. Mater.* **2000**, *12*, 359. (g) Lee, J.; Sohn, K.; Hyeon, T. *J. Am. Chem.* Soc. **2001**, *123*, 5146.
(4) Lee, J.-S.; Joo, S. H.; Ryoo, R. *J. Am. Chem. Soc.* **2002**, *124*, 1156.
(5) (a) Kim, T.-W.; Park, I.-S.; Ryoo, R. *Angew. Chem., Int. Ed.* **2003**, *42*, 4375. (b) Kim, C. H.; Lee, D.-K.; Pinnavaia, T. J. *Langmuir* **2004**, *20*, 5157.
(6) (a) Nam, J.-H.; Jang, Y.-Y.; Kwon, Y.-U.; Nam, J.-D. *Electrochem. Commun.* **2004**, *6*, 737. (b) Ding, J.; Chan, K.-Y.; Ren, J.; Xiao, F.-S. *Electrochim. Acta* **2005**, *50*, 3131. (c) Su, F.; Zeng, J.; Bao, X.; Yu, Y.; Lee, J. Y.; Zhao, X. S. *Chem. Mater.* **2005**, *17*, 3960. (d) Pak, C.; You, D. J.; Lee, S.-A.; Kim, J. M.; Chang, H. *Samsung J. Innovative Technol.* **2005**, *1*, 239.
(7) (a) Yoon, S.; Lee, J.; Hyeon, T.; Oh, S. M. *J. Electrochem. Soc.* **2000**, *147*, 2507. (b) Zhou, H.; Zhu, S.; Hibino, M.; Honma, I.; Ichihara, M. *Adv. Mater.* **2003**, *15*, 2107.
(8) (a) Vinu, A.; Streb, C.; Murugesan, V.; Hartmann, M. *J. Phys. Chem. B* **2003**, *107*, 8297. (b) Vinu, A.; Chandrasekar, G.; Hartmann, M. *Chem. Mater.* **2005**, *17*, 829.
(9) (a) Kang, M.; Yi, S. H.; Lee, H. I.; Yie, J. E.; Kim, J. M. *Chem. Commun.* **2002**, 1944. (b) Lu, A.-H.; Schmidt, W.; Taguchi, A.; Spliethoff, B.; Tesche, B.; Schüth, F. *Angew. Chem., Int. Ed.* **2002**, *41*, 3489.
(10) Boehm, H. P. *Carbon* **1994**, *32*, 759.
(11) Kinoshita, K. *Carbon: Electrochemical and Physicochemical Properties*; Wiley-Interscience: New York, 1988.
(12) Radovic, L. R.; Rodriguez-Reinoso, F.; Thrower, P. A. *Chemistry and Physics of Carbon*; Marcel Dekker: New York, 1997; Vol. 25, p 243.
(13) Jun, S.; Choi, M.; Ryu, S.; Lee, H.-Y.; Ryoo, R. *Stud. Surf. Sci. Catal.* **2003**, *146*, 37.
(14) Li, Z.; Dai, S. *Chem. Mater.* **2005**, *17*, 1717.
(15) Li, Z.; Del Cul, G. D.; Yan, W.; Liang, C.; Dai, S. *J. Am. Chem. Soc.* **2004**, *126*, 12782.
(16) Choi, M.; Ryoo, R. *Nat. Mater.* **2003**, *2*, 473.
(17) Kim, C. H.; Kim, S.-S.; Guo, F.; Hogan, T. P.; Pinnavaia, T. J. *Adv. Mater.* **2004**, *16*, 736.
(18) Kim, S.-S.; Foley, T. R.; Pinnavaia, T. J. *Chem. Commun.* **2000**, 1661.
(19) Kaden, H.; Jahn, H.; Berthold, M. *Solid State Ionics* **2004**, *169*, 129.
(20) Yang, C.-M.; Weidenthaler, C.; Spliethoff, B.; Mayanna, M.; Schüth, F. *Chem. Mater.* **2005**, *17*, 355.
(21) HiSPEC Catalyst Customer Chart (http://www.jmfuelcells.com/HiSPEC_Customer_Chart.pdf).
(22) Lee, S. J.; Mukerjee, S.; McBreen, J.; Rho, Y. W.; Kho, Y. T.; Lee, T. H. *Electrochim. Acta* **1998**, *43*, 3693.
(23) Aricò, A.; Cretì, P.; Kim, H.; Mantegna, R.; Giordano, N.; Antonucci, V. *J. Electrochem. Soc.* **1996**, *143*, 3950.